Flow Field Visualization of Entangled Polybutadiene Solutions under Nonlinear Viscoelastic Flow Conditions

Yanfei Li, Miao Hu, and Gregory B. McKenna[a)]

Department of Chemical Engineering, Texas Tech University, Lubbock, TX 79409, United States

Christopher J. Dimitriou, and Gareth H. McKinley

Department of Mechanical Engineering, Massachusetts Institute of Technology, Cambridge, MA 02139, United States

Rebecca M. Mick, and David C. Venerus

Department of Chemical and Biological Engineering and Center of Excellence in Polymer Science and Engineering, Illinois Institute of Technology, Chicago, IL 60616, United States

Lynden A. Archer

School of Chemical & Biomolecular Engineering and Department of Physics, Cornell University, Ithaca, NY 14853, United States

{Version of November 29, 2012}

Synopsis

Using self-designed particle visualization instrumentation, startup shear and step strain tests were conducted under a series of systematically varied rheological and geometrical conditions, and the velocity profiles of three different well-entangled polybutadiene/oligomer solutions were obtained. For startup shear tests, in the regime of entanglement densities up to 89 and Weissenberg numbers up to 18.6, we generally observe either wall slip and a linear velocity/strain profile or simply the linear profile with no wall slip unless a massive edge fracture or instability has occurred in the sample. Meanwhile, step strain tests were conducted under similar and higher step Weissenberg numbers, and little motion was observed upon cessation. These results lead us to a conclusion that there is no compelling evidence of shear banding or non-quiescent relaxation in the range of entanglement density and Wi investigated; we interpret the results to imply that any observed banding probably correlates with edge effects, and these probably are also present in the work of the S. Q. Wang group, and they lead to shear banding.

[a)]Author to whom correspondence should be addressed; electronic mail: greg.mckenna@ttu.edu

I. INTRODUCTION

The rheology of entangled polymer melts and solutions has been a subject of intensive research and, it was thought, a fairly well resolved problem because of the development of the tube model [Doi and Edwards (1978a, 1978b, 1978c, 1979); de Gennes (1971)] in the late 1970s. In the original version of this model Doi and Edwards (DE) (1978a) proposed that a test chain, moving in a snake-like fashion, is constrained by its surrounding segments by forming entanglements with them. Based on this assumption, the DE theory has shown reasonable agreement with experimental findings [Graessley (1980); Kremer and Grest (1990)], and has become the current paradigm in the community, although discrepancies with experimental evidence have been found especially when being applied to the nonlinear viscoelastic (NLVE) regime. A well-known failure of the DE theory lies in its inability to predict the experimentally observed monotonic steady state constitutive relationship between shear stress and shear rate [Doi and Edwards (1979)]. Specifically, if the constitutive curve indeed is non-monotonic as predicted by the DE model, shear banding should occur, meaning that bands with different shear rates could form in the sample above a critical shear stress or shear rate; however, this non-monotonicity or shear banding has not been normally observed [Hu (2010); Hayes et al. (2008)]. On the other hand, in step strain tests, it was found that the DE model underestimates the strain softening behavior in some cases [Osaki and Kurata (1980); Vrentas and Graessley (1982)]. In brief, the DE model predicts a universal form of damping function $h(\gamma)$, which measures the isochronal ratio of the NLVE relaxation modulus $G(t,\gamma)$ and its counterpart in the linear regime $G(t)$ (larger than $G(t,\gamma)$ due to softening), provided that time and strain are separable. Although in some cases agreement has been found between the prediction of the DE model and experiments [Osaki et al. (1982)], there are instances in which a "type-C" excessive strain softening (the feature of interest being that the observed damping function lies below the DE model prediction) has been reported.

Regarding the validity of the non-monotonic constitutive curve, the popular viewpoint [Marrucci (1996); Ianniruberto and Marrucci (2001); Graham et al. (2003)] is that it is a theoretical artifact in the DE model that leads to this discrepancy, and additional physics such as convective constraint release [Marrucci (1996)] needs to be taken into account. Furthermore, interfacial slippage has been proposed to be responsible for the type-C damping function [Juliani and Archer (2001); Sanchez-Reyes and Archer (2002); Archer et al. (2002); Venerus and Nair (2006)]. Fairly speaking, these efforts based on the DE model have been able to provide better agreement with experiment, implying that the DE model, while it has some defects, captures the essential underlying physics of entangled polymer systems.

Nevertheless, it is important to realize that material properties, either those predicted by the tube models or calculated from rheometric measurements, are obtained based on the assumption that during flow or deformation the samples stay intact, i.e., the flow or deformation field should be homogeneous [Ferry (1980)]. To examine the validity of this basic assumption, there has been much work published during the past decade, among which those reported by Wang and co-workers are the most important and intriguing [Tapadia and Wang (2003, 2004, 2006); Ravindranath and Wang (2007, 2008); Ravindranath et al. (2008); Boukany and Wang (2007, 2009a); Wang et al. (2011); Cheng and Wang (2012)]. By using particle tracking velocimetry (PTV), Ravindranath et al. (2008) observed shear banding behavior during startup shear tests, which is illustrated in Figure 1a where we see that velocity profiles during a startup shear are nonlinear. Ravindranath and Wang (2007) also found what they referred to as "non-quiescent relaxation" in step strain tests, meaning the bulk of the sample does not remain motionless while relaxing;

instead, it moves by forming bands or recoiling, as shown in Figure 1b. As an explanation for these phenomena, Ravindranath et al. (2008) attributed both shear banding and non-quiescent relaxation to "elastic yielding", which is a microscopic failure occurring in the bulk of the material under a large and abrupt strain. If such findings are universally valid, not only would the reptation models become unsupported by rheometric measurements, but also a significant amount of nonlinear rheology in polymer melts and solutions [Zapas and Craft (1965); Osaki et al. (1981, 1993, 2000); Pearson and Rochefort (1982); Venerus and Kahvand (1994); Reimers and Dealy (1996); Hyun et al. (1999); Sui and McKenna (2007)] would need to be reevaluated. Hence, the purpose of the present collaborative research has been to assess the validity of the results reported by Wang and co-workers.

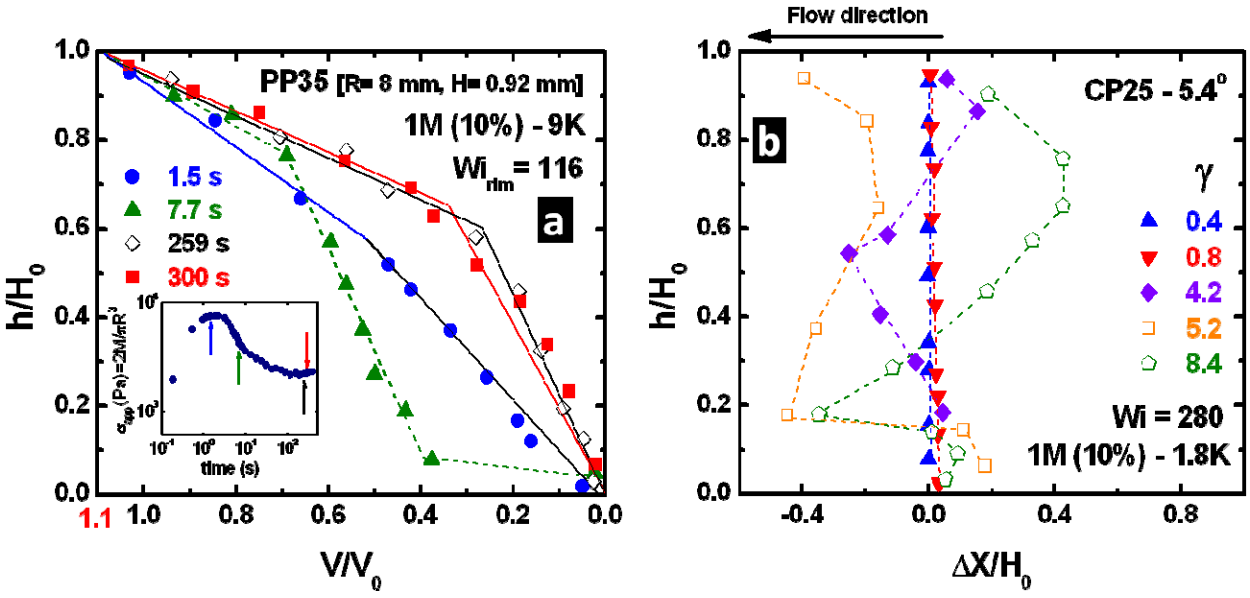

Figure 1. (a) A representative figure showing shear banding at an apparent Wi of 116. Vertical axis represents position in gap of rheometer and horizontal axis is the velocity at that position. Note that the "R" specified in the figure indicates the laser position. It is interesting to note that the data points near the moving surface actually have velocity values larger than the imposed velocity at the platen. (After [x]). (b) A representative figure showing non-quiescent relaxation upon the cessation of shear for different strain magnitudes. H is position across gap and ΔX is the displacement as measured by particle tracking velocimetry. (After [x]). Data in both figures were digitized from the original paper.

To decipher the mystery, a group of rheologists was brought together to carry out independent particle tracking and imaging velocimetry in conditions that nominally fall into Wang's shear banding "phase diagram" [Wang et al. (2011)] (shown subsequently), which maps the conditions of entanglement density and Weissenberg number that would show a linear profile, wall slip or shear banding instabilities. In cases where wall slip is a concern, platens were chemically treated to successfully minimize the slippage. As shown subsequently, shear banding and non-quiescent relaxation were not detected, unless edge effects become dominant, which seems to support the recent findings that edge instability can initiate the occurrence of flow instability [Inn et al. (2005); Sui and McKenna (2007)].

II. EXPERIMENTAL

A. Materials

The polymer solutions studied were mixtures of cis-1, 4 polybutadienes (PBD) of high molecular weights (Polymer Source Inc.) and phenyl terminated oligomeric polybutadienes (Sigma-Aldrich Corp.). To prepare the samples, a high-molecular-weight PBD was first dissolved in toluene for three days. After that, the oligomeric PBD was added, along with 0.5 phr of butylated hydroxytoluene as an antioxidant. After most of the toluene evaporated, the sample container was placed under vacuum until the residual toluene became less than 0.5 % of the total weight of the sample. For the particle tracking experiments, 0.1 phr of silver-coated particles of diameters between 2-20 μm (Dantec Dynamics HGS-10) were mixed by gently stirring into the sample to obtain a homogeneous system. For the purpose of particle imaging, a trace amount of TiO_2 particles of 3-5 μm were mixed with the sample. Following this protocol, three different samples with different molecular weights and concentrations were made, the compositions and properties of which are listed in Table 1.

Table 1. Compositions and properties of the samples

sample name	1M10% - 1.5K	1.4M10% - 9K	1.4M15% - 1.5K
[a] M_w (g mol $^{-1}$) x 10^3	1,060	1,400	1,400
[a] M_n (g mol $^{-1}$) x 10^3	960	1,200	1,200
[a] oligomer M_n (g mol $^{-1}$) x 10^3	1.5	9.0	1.5
Mass concentration ϕ (%)	10.0	10.0	15.0
[b] entanglement density $Z(\phi)$	42	55	89
[c] sample viscosity η_o (Pa.s)	4,300	300,000	210,000
[c] solvent viscosity η_s (Pa.s)	0.8	12.1	0.8
[c] terminal relaxation time τ_d (s)	1.4	119.4	60.5
[d] extrapolation length b_{max} (mm)	0.1	0.4	3.1

[a] Molecular weights of the polybutadiene samples and the oligomers were provided and guaranteed by Polymer Source, Inc. and Sigma-Aldrich Corp., respectively.

[b] Entanglement density $Z(\phi)$ was calculated as $Z(\phi) = M_w/M_e(\phi) = M_w/ (M_e*\phi^{-1.2})$, where the entanglement density M_e for polybutadiene melts is taken as 1,600 g mol $^{-1}$.

[c] The zero shear viscosity of the samples η_o and the solvents η_s were measured at 25 ^oC by taking the steady state values of startup shear tests at Weissenberg numbers much smaller than unity, and the terminal relaxation times were calculated as $\tau_d = 1/\omega_c$, where ω_c (in rad/s) is the crossover frequency in a frequency sweep test.

[d] The theoretical maximum extrapolation length b_{max} was calculated according to the Appendix A of [Wang et al. (2011)] (actual extrapolation length b is smaller than b_{max}, and this is especially true when surface is treated).

B. Instrumentation

Particle tracking and particle imaging velocimeters were designed and constructed in the TTU and MIT laboratories, respectively. Although both set-ups were designed to work on the AR-G2 rheometer (TA Instruments), they are based on different geometries as described in what follows. In addition, laboratories at Cornell and IIT made their respective confocal microscopy and classical rheometry capabilities available.

MIT particle imaging device: as shown in Figure 2 (a), a particle imaging (PIV) device is attached to an AR-G2 rotary rheometer. A cone and plate fixture with 50 mm diameter and 4 degree cone angle is used for this set-up. The upper platen is bare glass, and the lower cone is stainless steel painted by a thin layer of carbon black to suppress laser reflection. The incident angle of the laser is about 45 degrees, and a CCD camera with a frame rate of 60 fps looks through a narrow glass window at an angle of 45 degrees. The results shown in Figures 4 and 5, subsequently, were obtained with this set-up.

TTU particle tracking device: based on a similar idea, a self-designed particle tracking (PTV) device was attached to an AR-G2. In this set-up, the beam of a 10 mW He-Ne laser travels through an optical system consisting of a mirror, a slit, and two orthogonally placed cylindrical convex lenses, and enters the sample at an angle of 45 degrees. By using this optical combination, the cross-sectional area of the laser travelling in the sample is reduced to about 0.1 mm x 3 mm. The movement of the illuminated particles is recorded by a CCD camera (15 fps) through the bottom platen by using another mirror. The glassy parallel platens have a diameter of 25 mm and the laser sheet can move freely along the radius. All measurements were performed at room temperature. Under some circumstances, to probe the effects of edge-wrapping, a plastic wrap was placed around the edge of the platens with a clearance of 0.5 mm in between the plastic wrapping and the edge of the platen/sample.

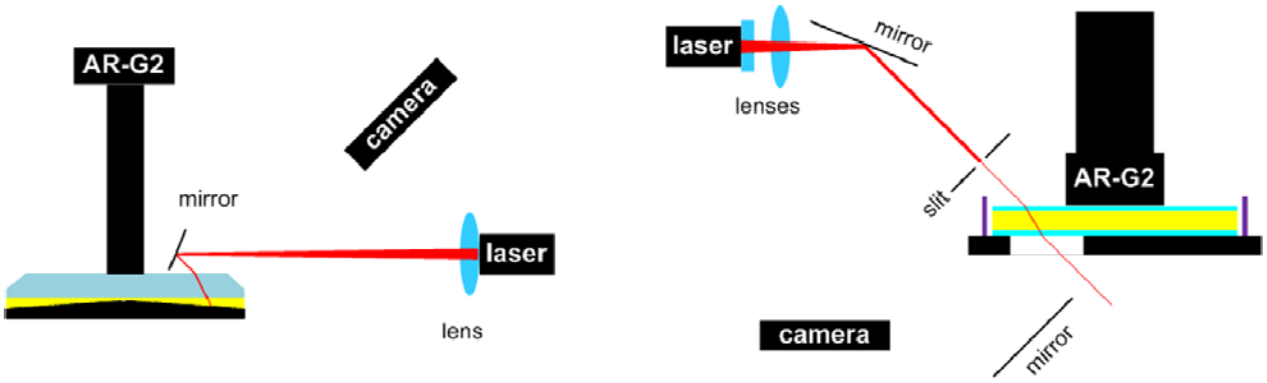

Figure 2. Schematics of **(a)** Particle imaging velocimeter at MIT. **(b)** Particle tracking velocimeter at TTU.

C. Surface treatment of the substrates (TTU)

Because surface slippage is a concern in nonlinear rheometry, it is interesting to compare experiments with bare glass surfaces as well as those in which the surfaces were chemically treated to suppress slippage. To do the surface treatment, a layer of (3-acryloxypropyl) trimethoxysilane (a silane coupling

agent with a double bond on the hydrophobic end) was chemically attached to the glass platens used in the rheometer. Subsequently, a polybutadiene/dicumyl peroxide mixture (1.0 phr) dissolved in toluene was coated on top of the pretreated substrates. Upon drying the PBD formed a layer of approximately 4 μm thickness (estimated from the total volume and concentration of PBD solution). Substrates were then heated at 130 ^{o}C under nitrogen protection for approximately six hours to react the peroxide sufficiently to reach the gel point. In this way, by creating a lightly crosslinked layer of PBD, the chains in the PBD solutions can interpenetrate the rubber (network) layer and, consequently, wall slip was successfully suppressed, as shown later.

III. RESULTS AND DISCUSSION

A. Phase diagram

Wang et al published a phase diagram showing the correlations between velocity profiles and material properties, shear rates, and geometric factors. The detailed theory involved in deriving this phase diagram is explained in Wang's roadmap paper of 2011 [Wang et al. (2011)]. In Figure 3, we replicate Wang's phase diagram and enhance it by placing the tests discussed in the present work onto it. In brief, the whole phase diagram can be divided into four regions, and the signature of the velocity profile in each region is indicated accordingly. It is worth pointing out that the apparent dividing line between wall slip and shear banding (dashed line) applies only upon complete chain disentanglement at the interface. As long as wall slippage is minimized by using the strategy described above, the true dividing line should approach the red horizontal phase line [Wang et al. (2011)]. By realizing this, it is safe to say that most tests in this study are well within the shear banding regime. As a reference, the startup shear and step strain tests by Wang et al shown in the introduction are placed onto this phase diagram as well, indicated as "a" and "b", respectively.

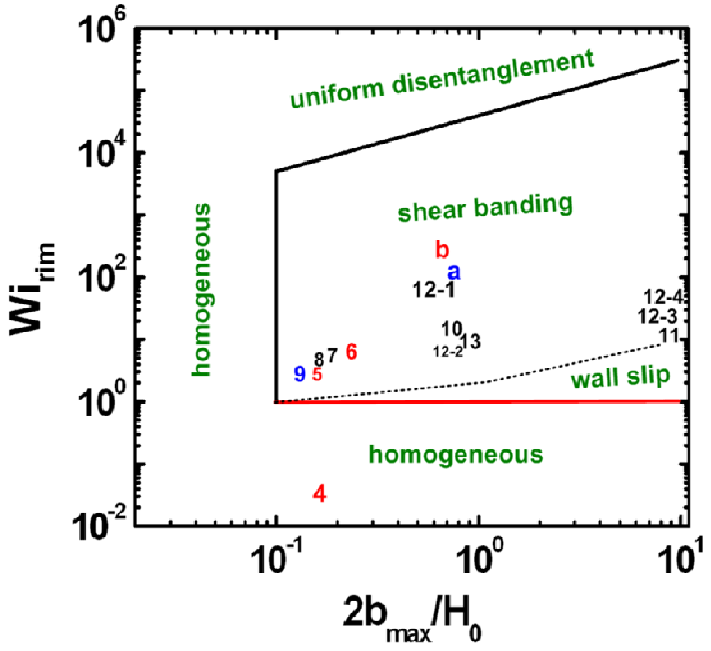

Figure 3. Phase diagram derived from reference [x] for velocity profiles in the parameter space of applied Weissenberg number and $2b_{max}/H_o$. Note that the numbers in the phase diagram indicate test numbers in the present work, and test numbers are referred to as the black highlighted numbers in each figure presented in the "results and discussion" section. Numbers in this phase diagram are colored to mean the following: red means no surface treatment (bare glass), black means with surface treatment (polybutadiene film attached to the platen surfaces to suppress slip), and blue means plastic wrapped around edge of platens (with surface treatment).

B. Startup shear of 1M10%-1.5K

This section is focused on the velocity profiles during startup shear for the 1M10%-1.5K solution, which has approximately 42 entanglements per chain. It is well-recognized that polymer solutions should maintain a linear velocity profile as long as the shear rate is sufficiently low such that Wi<< 1. Therefore, a startup shear test was conducted at a value of Wi= 0.03, and the steady state velocity profile is displayed in Figure 4. It is obvious that the velocity profile remains linear without any signature of wall slip.

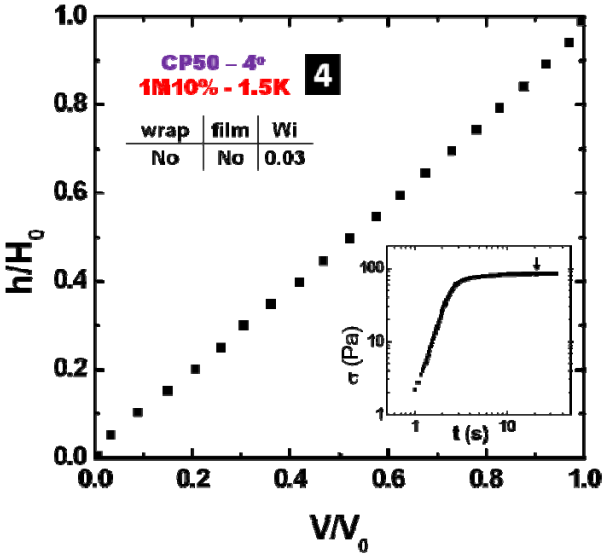

Figure 4. Velocity profiles during the steady state of a startup shear at a nominal Weissenberg number of 0.03. The sample 1M10% - 1.5K is tested by using the MIT PIV set-up that is coupled with a CP50 – 4° geometry (cone plate with a diameter of 50 mm and a cone angle of 4°). The inset shows the shear stress development during the startup shear, and the arrow specifies the time point at which velocity profiles are analyzed. The table in the figure indicates that the edge of the sample is in direct contact with air, and the surface is bare glass (not chemically treated). The black-highlighted number "4" is the test number of this test, which corresponds to the number "4" in the diagram in Figure 3.

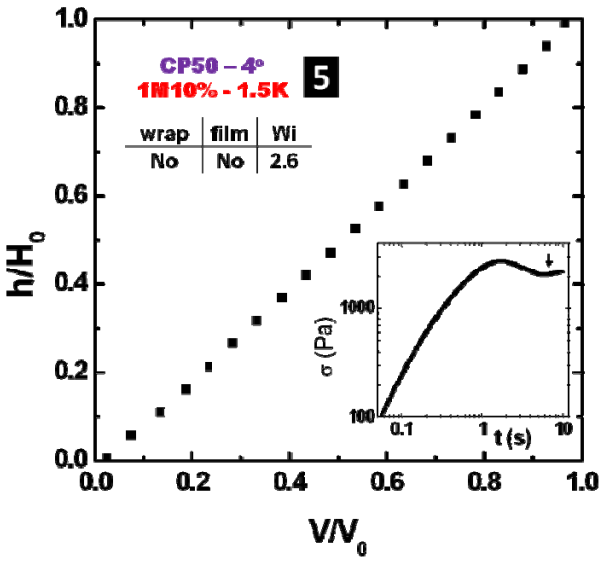

Figure 5. Velocity profiles during the steady state of a startup shear at a nominal Weissenberg number of 2.6.

However, when the Wi is increased to 2.6, as seen in Figure 5, although the steady state velocity curve is still linear, there is about 3 % slippage at both platens. Remark that the test 5 situated in the shear banding regime of the phase diagram of Figure 3 is close to the "phase line" between slip and shear banding. Therefore, tests at higher Wi were carried out to obtain results deeper into the shear banding regime.

To this end, in Figure 6, a pair of bare glass platens was used and a Wi of 6.4 was applied to the sample. Obviously, the velocity profiles remain linear with about 10 % wall slip at both platens. It is important to notice that even by considering the loss of shear rate due to wall slip, the net Wi in the bulk is still high enough so that this solution is into the shear banding regime of the phase diagram.

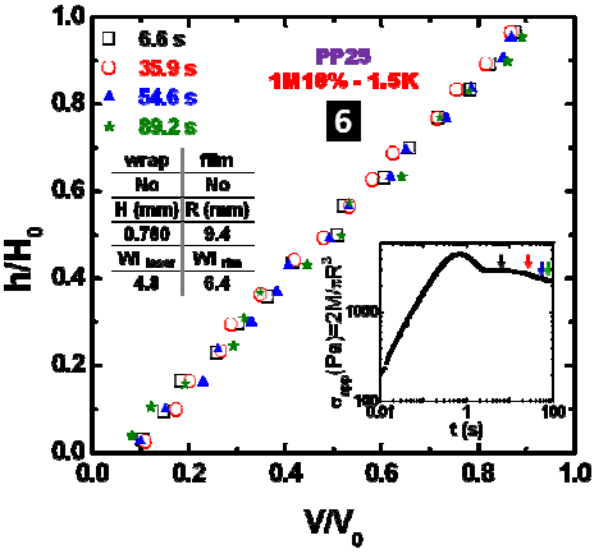

Figure 6. Velocity profiles during a startup shear at a nominal Weissenberg number of 6.4. The "R" in the table in the figure indicates the distance of the laser from the center, and the Weissenberg numbers at both the laser and the rim are shown in the table.

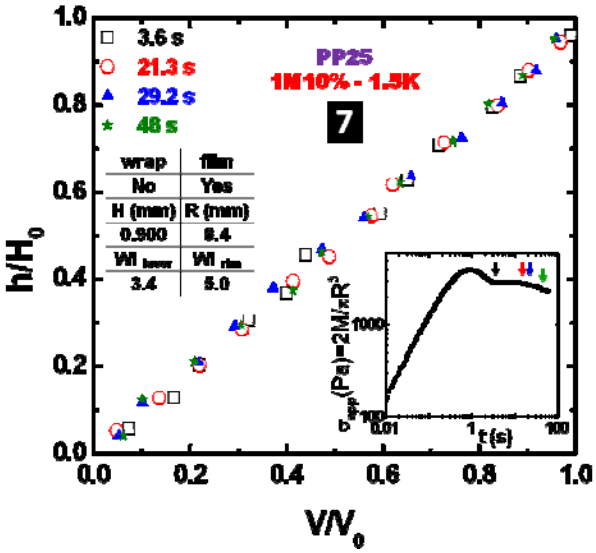

Figure 7. Velocity profiles during a startup shear at a nominal Weissenberg number of 5.0 for sample that is tested with platens treated to suppress wall slip.

Boukany and Wang (2009b) attributed the occurrence of wall slip to "interfacial yielding", which is a manifestation of shear banding happening at the interface as long as the chains adsorbed are not as entangled as those in the bulk. This argument, if true, implies that the observed wall slip in Figure 5 and 6 might actually be a demonstration of "interfacial shear banding". Therefore, it was important for us to suppress wall slip/interfacial yielding in order to deconvolute it from the examination of shear banding. To do so, we followed the surface modification protocol described in the experimental section, and another startup shear experiment with Wi= 5.0 was carried out with the results shown in Figure 7. As can be seen, the velocity profile is still linear and the wall slip is effectively suppressed.

An alternative way of examining the effectiveness of the surface treatment is to compare the rheological responses under two similar nominal shear rates, but with different surfaces. To be specific, one test is under a somewhat higher nominal Wi of 1.63, with the platen surface as bare glass, and the other was performed using the chemically modified surfaces and at a slightly lower Wi of 1.55. Here we did not show the results in a figure, but the key observation is that the test at the lower shear rate gives an approximately 5 % higher steady state shear stress. Neglecting the shear thinning effects, the slipping magnitudes at both surfaces would be 5.8 %; however, with shear thinning taken into account, this value approaches zero, which is consistent with the finding in Figure 7.

The results above suggest that there is no shear banding in the regime near the lower left corner of the phase diagram of Figure 3 where shear banding should occur. Hence, one can raise the question as to

whether Wang's observations, e.g., in Figure 1, were due to an edge effect. This can be especially problematic when the gap is large, or when the laser sheet is brought too close to the edge of the platens, or when an edge-wrapping approach is applied, as was sometimes done in Wang's laboratories [Ravindranath and Wang (2008); Ravindranath et al. (2008)].

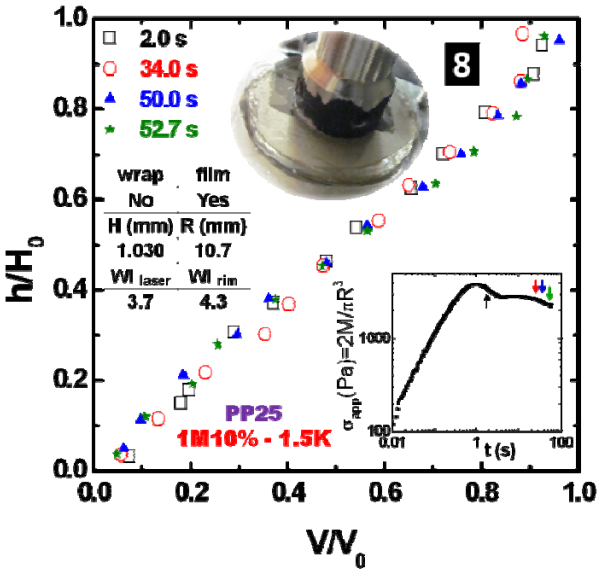

Figure 8. Velocity profiles during a startup shear at a nominal Weissenberg number of 4.3. The inset shows image of the shearing cell immediately after the cessation flow and evidences edge fracture. Notice that gap is somewhat larger than prior figures and the laser position is nearer to the edge of the platens.

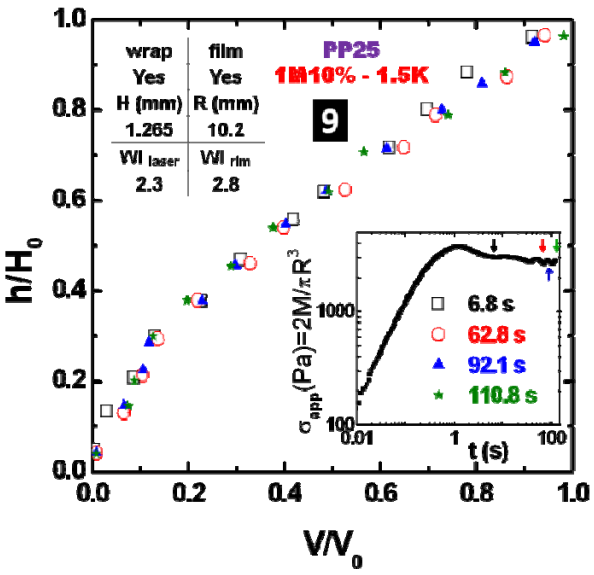

Figure 9. Velocity profiles during a startup shear at a nominal Weissenberg number of 2.8 for a sample with plastic sheet around the edge of the sample.

In order to examine the influences of the gap and laser position on the velocity profile, a combination of larger gap and radial position of the laser was used in another startup shear test. We see evidence in Figure 8 for Wi values similar to those of Figure 7 (but with somewhat larger gap and a laser sheet position nearer to the edge of the platens) of flow instability. Specifically, the velocity profile is no longer linear at all times in the flow, i.e., the velocity profile switches between being linear and being banded (Compare 2 s profile with 34 s profile, for example). Compared with Figure 7, where the profiles remain linear, it seems that this transient banding phenomenon is due to the fact of the larger gap and the position of the laser sheet being closer to the platen edge. Our explanation is that the sample is exposed to a sufficiently high shear rate and either edge fracture or other edge instability occurs. This leads to an irregular flow field near to the sample edge which propagates slowly inwards towards the center of the sample and distorts the velocity field, perhaps randomly. In our current set-up, it is difficult to quantify the depth of the transmission of this irregular flow field. But, from the inset of Figure 8, the depth of the edge distortion is estimated to be more than 1 mm and hence the irregular flow field is probably deeper than 1 mm. Since it is in conditions such as these that we see shear banding, and not nearly as severe as that observed by Wang's group, it is fair to say that for this sample any observed banding is due to edge instability.

Wang and co-workers did understand that edge instability could lead to problems in the flow field development and used two methods to help either prevent sample loss due to edge instabilities or simply

eliminate their visual appearance. They used either a plastic wrap or a cone-partitioned plate device [Ravindranath and Wang (2008); Ravindranath et al. (2008)]. These two set-ups look different, but the basic ideas are the same, which is to suppress edge fracture or instability during the tests. The evidence from Figure 8 that transient shear banding can be geometry-related led us to examine the influence on the "internal" flow field of putting a plastic wrap around the sample edge. Figure 9 shows a similar experiment to that of Figure 8, except that, now there is a plastic wrap on the sample. We find that the velocity profile remains curved throughout the entire test even though the overall shear rate at the rim is somewhat lower than that used for the experiment of Figure 8. Therefore, it is reasonable to conclude that the wrap, while it succeeds in suppressing the visual appearance of edge instability, complicates the internal flow field during startup shear. Importantly, in the samples with narrower gaps but similar and higher Wi (Figures 5-7), there is no evidence of shear banding without the wrap. It is necessary to mention that we also tried to compare the torque as a function of time during startup shears under similar shear rates, and the experiment with the plastic wrap turned out to have an obviously higher torque than that without the wrap, which contradicts Wang's finding that edge-protection elements do not change the rheological response. Hence, it appears that the edge instability is only changed in nature by the presence of the plastic sheet, but not eliminated.

C. Startup shear of 1.4M10% - 9K and 1.4M15% - 1.5K

In order to move the position of the material studied further into the shear banding regime of Figure 3 we made another solution 1.4M10% - 9K using both a higher molecular weight solvent and a higher molecular weight polymer. This both increases the entanglement density somewhat and changes the slip length b_{max}, which Wang considers important in the "phase diagram". In addition we considered a sample 1.4M15% - 1.5K of higher molecular weight and concentration, but the lower molecular weight oligomeric solvent. Typical velocity profiles for these two samples are shown in Figures 10 and 11, respectively. The figures show no significant heterogeneity in the flow fields, again contradicting the results reported by Wang's group. Also, edge rupture was observed at the end of these two tests, and the magnitude of this rupture is similar to that observed for the 1M10% - 1.5K at a similar Weissenburg number; however, for some reason, the velocity profiles of these two more viscous samples were not affected by the edge effects too much, probably either because the gap used was somewhat narrow (1mm and 0.65 mm, respectively) or the laser sheet was not placed sufficiently close to the edge to sense the fracture.

D. Relaxation after imposed shear

Recalling Figure 1b, we also examined the apparent flow instabilities induced by experiments in which the rapid shear is stopped and the sample is allowed to relax. Wang's group reported a recoil event in which the strains were heterogeneous. In order to test this, we carried out such "step strain" tests under different strain rates and strain magnitudes using the 1.4M10% - 9K and 1.4M15% - 1.5K materials. Particle tracking images were taken up to 5,000 seconds after the cessation of shear, and no motion was ever observed in the samples (zero displacement). Figure 12 gives an example of a system well into the nominal shear banding/recoil regime but that shows no anomalous motion. This was true for all of the step-strain types of experiments we performed that are summarized in Table 2. It is important to note that those tests also were well into the shear banding regime in the phase diagram of Figure 3.

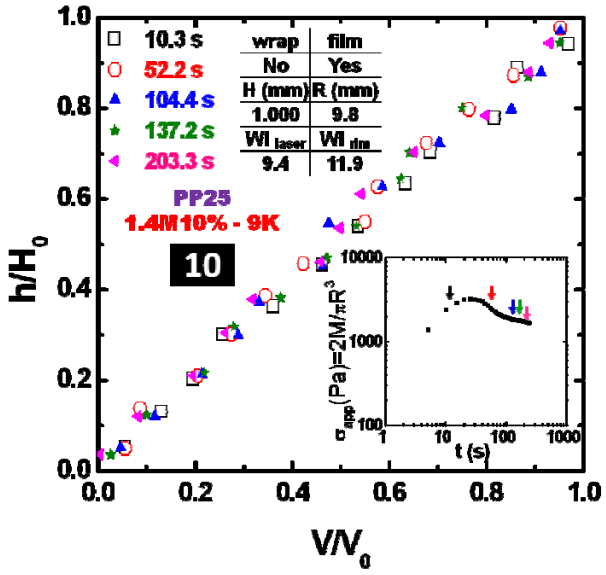

Figure 10. Velocity profiles during a startup shear at a nominal Weissenberg number of 11.9 for high molecular weight with highly viscous oligomeric solvent.

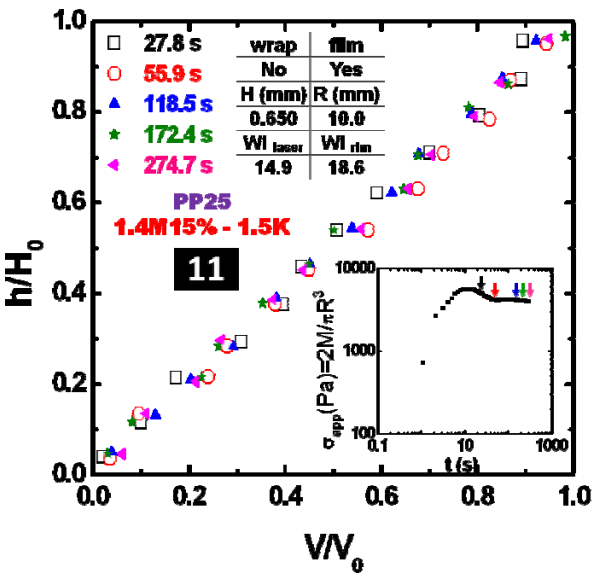

Figure 11. Velocity profiles during a startup shear at a nominal Weissenberg number of 18.6 for the high molecular weight polymer at 15% concentration in the low molecular weight oligomeric solvent.

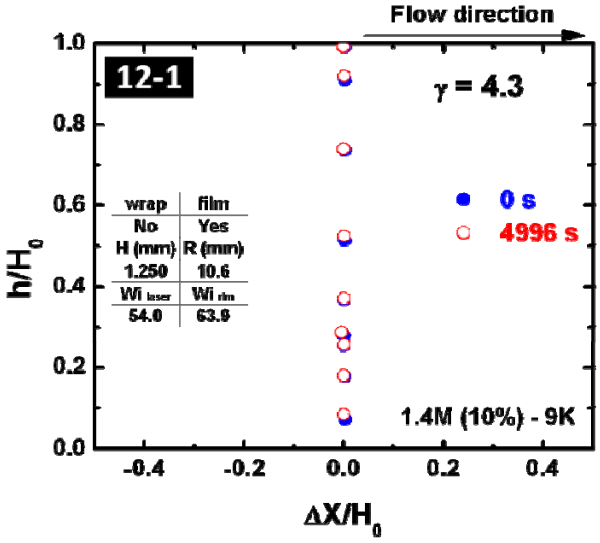

Figure 12. Displacement profile for step-strain condition showing no anomalous recoil.

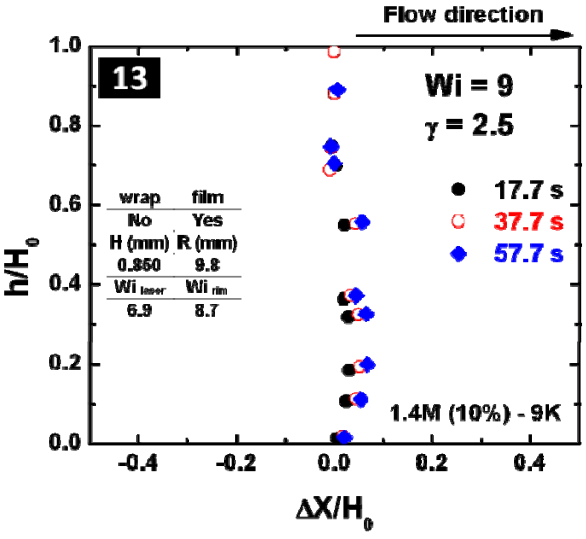

Figure 13. Displacement profile for step-strain condition of an intentionally misaligned platens that shows apparent anomalous elastic recoil.

In addition to the experiments in step strain in which we saw no unusual displacements, we also performed an experiment in which we purposely misaligned the platens slightly (visually less than 0.1 mm) and the results of this experiment are shown in Figure 13. There we see for the misaligned system,

there is an apparent movement during the relaxation step. However, the magnitude of this motion still is not as great as that in Figure 1b.

Table 2. Test conditions for step strain tests (none of them shows non-quiescent relaxation)

Test #	Laser position R (mm)	H (mm)	Wi_{rim}	γ_{rim}
12-1	10.6	1.250	63.9	4.3
12-2	9.7	1.000	7.5	2.2
12-3	10.0	0.738	18.9	4.1
12-4	10.0	0.612	37.8	6.3

IV. SUMMARY

Three highly entangled polymeric solutions were studied using PIV and PTV techniques to understand the startup shear and step strain behaviors in the nonlinear viscoelastic regime and, specifically, to investigate the regime of validity of the reported shear banding in nonlinear flows from the S.Q. Wang group. On bare glass substrates, 1M10%-1.5K features a linear velocity profile with interfacial slippage during a startup shear. However, when substrates are treated with crosslinked rubber films, wall slip can be effectively eliminated. When edge effects become important, velocity profiles become unstable and randomly switch between being linear and being slightly sigmoid-like. We also observed a consistently curved profile when both a plastic sheet was wrapped around the sample edge and the slip-prevention "films" were applied to the platens. Importantly, in nearly all cases with sufficiently narrow gap, even when well within the "phase diagram" region where shear banding should occur, we did not observe shear banding. Equally important, compared with the large magnitude of motion during step strain relaxation observed by Wang and co-workers, no motion was observed for the two highly entangled samples considered in the present work. Finally, we were able to observe apparent elastic recoil in the step-strain type of experiment when platens were intentionally misaligned, suggesting that misalignment might be one source of the apparent shear banding and recoil events reported by Wang's group.

Although we have not been able to reproduce Wang's findings, there are certain things that it is worth reminding the community that may require special attention in performing nonlinear rheological experiments on polymer melts and solutions: 1) wall slip needs to be suppressed by appropriate surface treatment when possible to obtain the correct rheological properties; 2) edge effects should be minimized as much as possible by, for example, using a relatively small gap; 3) platens should be aligned well to avoid any possible abnormal flow behavior; 4) the advances in PIV or PTV make possible verification of the experimental flow/deformation field and should be used when possible.

ACKNOWLEDGEMENTS

The authors are thankful to the National Science Foundation under grant DMR–0934305 for support of this work. The authors from TTU also thank the John R. Bradford Endowment for partial support.

References

Archer, L. A., J. Sanchez-Reyes, and Juliani, "Relaxation Dynamics of Polymer Liquids in Nonlinear Step Shear," Macromolecules **35**, 10216–10224 (2002).

Boukany, P. E., and S. Wang, “A Correlation Between Velocity Profile and Molecular Weight Distribution in Sheared Entangled Polymer Solutions," J. Rheol. **51**, 217–233 (2007).

Boukany, P. E., and S. Wang, “Shear Banding or not in Entangled DNA Solutions Depending on the Level of Entanglement," J. Rheol. **53**, 73–83 (2009).

Boukany, P. E., and S. Q. Wang, “Exploring Origins of Interfacial Yielding and Wall Slip in Entangled Linear Melts during Shear or after Shear Cessation,” Macromolecules **42**, 2222–2228 (2009).

Cheng, S., and S. Wang, “Is Shear Banding a Metastable Property of Well-Entangled Polymer Solutions?," J. Rheol. **56**, 1413–1428 (2012).

de Gennes, P.G., “Reptation of a Polymer Chain in the Presence of Fixed Obstacles,” J. Chem. Phys. **55**, 572–579 (1971).

Doi, M., and S. F. Edwards, “Dynamics of Concentrated Polymer Systems Part 1.–Brownian Motion in the Equilibrium State,” J. Chem. Soc. Faraday Trans. 2 **74**, 1789–1801 (1978).

Doi, M., and S. F. Edwards, “Dynamics of Concentrated Polymer Systems Part 2.-Molecular Motion under Flow,” J. Chem. Soc. Faraday Trans. 2, **74**, 1802–1817 (1978).

Doi, M., and S. F. Edwards, “Dynamics of Concentrated Polymer Systems Part 3.-The Constitutive Equation,” J. Chem. Soc. Faraday Trans. 2, **74**, 1818–1832 (1978).

Doi, M., and S. F. Edwards, “Dynamics of Concentrated Polymer Systems Part 4.–Rheological Properties,” J. Chem. Soc. Faraday Trans. 2, **75**, 38–54 (1979).

Ferry, J. D., *Viscoelastic Properties of Polymers* (Wiley, New York, 1980).

Graessley, W. W., “Some Phenomenological Consequences of the Doi-Edwards Theory of Viscoelasticity,” Journal of Polymer Science: Polymer Physics Edition **18**, 27–34 (1980).

Graham, R. S., A. E. Likhtman, and T. C. B. McLeish, “Microscopic Theory of Linear, Entangled Polymer Chains under Rapid Deformation Including Chain Stretch and Convective Constraint Release,” J. Rheol. **47**, 1171–1200 (2003).

Hayes, K. A., M. R. Buckley, I. Cohen, and L. A. Archer, "High Resolution Shear Profile Measurements in Entangled Polymers," Phys. Rev. Lett. **101**, 218301 (2008).

Hu, Y. T., “Steady-State Shear Banding in Entangled Polymers?,” J. Rheol. **54**, 1307–1323 (2010).

Hyun, K., M. Wilhelm, C. O. Klein, K.S. Cho, J. G. Nam, K. H. Ahn, S. J. Lee, R. H. Ewoldt, and G. H. McKinley, “A Review of Nonlinear Oscillatory Shear Tests: Analysis and Application of Large Amplitude Oscillatory Shear (LAOS),” Progress in Polymer Science **36**, 1697–1753 (2011).

Ianniruberto, G., and G. Marrucci, “A Simple Constitutive Equation for Entangled Polymers with Chain Stretch,” J. Rheol. **45**, 1305–1318 (2001).

Inn, Y. W., K. F. Wissbrun, and M. M. Denn, “Effect of Edge Fracture on Constant Torque Rheometry of Entangled Polymer Solutions,” Macromolecules **38**, 9385–9388 (2005).

Juliani, and L. A. Archer, “Linear and Nonlinear Rheology of Bidisperse Polymer Blends,” J. Rheol. **45**, 691–708 (2001).

Kremer, K., and G. S. Grest, “Dynamics of Entangled Linear Polymer Melts: A Molecular-Dynamics Simulation,” J. Chern. Phys. **92**, 5057–5086 (1990).

Marrucci, G., ‘‘Dynamics of entanglements: A Nonlinear Model Consistent with the Cox-Merz Rule,’’ J. Non-Newtonian Fluid Mech. **62**, 279–289 (1996).

Mhetar, V., and L. A. Archer, “Nonlinear Viscoelasticity of Entangled Polymeric Liquids,” J. Non-Newtonian Fluid Mech. **81**, 71-81 (1999).

Osaki, K., and M. Kurata, ‘‘Experimental Appraisal of the Doi-Edwards Theory for Polymer Rheology Based on the Data for Polystyrene Solutions,” Macromolecules **13**, 671–676 (1975).

Osaki, K., S. Kimura, and M. Kurata, “Relaxation of Shear and Normal Stress in Double-Step Shear Deformation for a Polystyrene Solution. A Test of the Doi and Edwards Theory for Polymer Rheology,” J. Rheol. **25**, 549–562 (1981).

Osaki, K., K. Nishizawa, and M. Kurata, “Material Time Constant Characterizing the Nonlinear Viscoelasticity of Entangled Polymeric Systems,” Macromolecules **15**, 1068–1071 (1982).

Osaki, K., “On the Damping Function of Shear Relaxation Modulus for Entangled Polymers,” Rheol. Acta **32**, 429-437 (1993).

Osaki, K., T. Inoue and T. Isomura, “Stress Overshoot of Polymer Solutions at High Rates of Shear,” J. Polym. Sci. Part B. Polymer Physics **38**, 1917-1925 (2000).

Pearson, D. S., and W. E. Rochefort, “Behavior of Concentrated Polystyrene Solutions in Large Amplitude Oscillating Shear Fields,” Journal of Polymer. Science: Part B: Polymer Physics **20**, 83-98 (1982).

Ravindranath, S., and S. Wang, “What Are the Origins of Stress Relaxation Behaviors in Step Shear of Entangled Polymer Solutions?,” Macromolecules **40**, 8031–8039 (2007).

Ravindranath, S., S. Wang, M. Olechnowicz, and R. Quirk, “Banding in Simple Steady Shear of Entangled Polymer Solutions,” Macromolecules **41**, 2663–2670 (2008).

Ravindranath, S., and S. Wang, “Steady State Measurements in Stress Plateau Region of Entangled Polymer Solutions: Controlled-Rate and Controlled–Stress Modes," J. Rheol. **52**, 957–980 (2008).

Reimers, M. J., and J. M. Dealy, “Sliding Plate Rheometer Studies of Concentrated Polystyrene Solutions: Large Amplitude Oscillatory Shear of a very High Molecular Weight Polymer in Diethyl Phthalate,” J. Rheol. **40**, 167-186 (1996)

Sanchez-Reyes, J., and L. A. Archer, “Step Shear Dynamics of Entangled Polymer Liquids,” Macromolecules **35**, 5194–5202 (2002).

Sui, C., and G. B. McKenna, “Instability of Entangled Polymers in Cone and Plate Rheometry,” Rheol. Acta **46**, 877–888 (2007).

Tapadia, P., and S. Wang, “Yieldlike Constitutive Transition in Shear Flow of Entangled Polymeric Fluids,” Phys. Rev. Lett. **91**, 198301 (2003).

Tapadia, P., and S. Wang, “Nonlinear Flow Behavior of Entangled Polymer Solutions: Yieldlike Entanglement−Disentanglement Transition,” Macromolecules **37**, 9083–9095 (2004).

Tapadia, P., and S. Wang, “Direct Visualization of Continuous Simple Shear in Non-Newtonian Polymeric Fluids," Phys. Rev. Lett. **96**, 016001 (2006).

Venerus, D. C., and H. Kahvand, “Doi and Edwards theory evaluation in double-step strain flows,” J. Polym.Sci., Part B: Polym. Phys. **32**, 1531–1542 (1994).

Venerus, D. C., and R. Nair, “Stress Relaxation Dynamics of an Entangled Polystyrene Solution Following Step Strain Flow,” J. Rheol. **50**, 59–75 (2006).

Vrentas, C. M., and W. W. Graessley, "Study of Shear Stress Relaxation in Well-Characterized Polymer Liquids," J. Rheol. **26**, 359–371 (1982)

Wang, S., S. Ravindranath and P.E. Boukany, “Homogeneous Shear, Wall Slip, and Shear Banding of Entangled Polymeric Liquids in Simple Shear Rheometry: A Roadmap of Nonlinear Rheology," Macromolecules **44**, 183–190 (2011).

Zapas, L. J., and T. Craft, “Correlation of Large Longitudinal Deformations with Different Strain Histories,” J. Res. National Bureau of Standards (U.S.) **69A**, 541-546 (1965).